Express Polymer Letters Vol.16, No.4 (2022) 439–450
Available online at www.expresspolymlett.com
https://doi.org/10.3144/expresspolymlett.2022.32

Research article

Fabrication and characterization of electrospun poly(3-aminobenzylamine)/functionalized multi-walled carbon nanotubes composite film for electrochemical glucose biosensor

Saengrawee Sriwichai[1,2*], *Sukon Phanichphant*[2]

[1]Department of Chemistry, Faculty of Science, Chiang Mai University, 50200 Chiang Mai, Thailand
[2]Center of Excellence in Materials Science and Technology, Chiang Mai University, 50200 Chiang Mai, Thailand

Received 1 October 2021; accepted in revised form 12 December 2021

Abstract. A glucose sensor has been developed for daily diagnosis due to high level of glucose can cause diabetes. This study purposes of fabricating an electrospun fiber film of poly(3-aminobenzylamine) (PABA)/functionalized multi-walled carbon nanotubes (f-CNTs) composite for use as electrochemical glucose biosensor. The electrospun PABA/f-CNTs composite film was fabricated on a screen-printed electrode and characterized by attenuated total reflectance-Fourier transform infrared spectroscopy (ATR-FTIR), X-ray diffraction (XRD) and X-ray photoelectron spectroscopy (XPS), and field emission–scanning electron microscopy (FE-SEM). The presence of f-CNTs in the composite could enhance the electrochemical activities of the PABA, which was confirmed by cyclic voltammetry (CV), amperometry, and electrochemical impedance spectroscopy (EIS). The electrochemical glucose biosensor based on the electrospun PABA/f-CNTs composite film showed a sensitivity of 0.40 $\mu A \cdot mm^{-2} \cdot mM^{-1}$ with LOD of 0.067 mM in the linear range of 0.56–2.8 mM, high selectivity under the common interferences (*i.e.*, uric acid, ascorbic acid, and dopamine) and good stability up to 1 week with the current response retained about 80%.

Keywords: *polymer composites, poly(3-aminobenzylamine), carbon nanotube, conducting polymer, biosensor*

1. Introduction

Conducting polymers such as polyaniline, polypyrrole, polythiophene, and their derivatives have been widely studied and applied in various applications, including biosensors and chemical sensors [1–4], batteries, and supercapacitors [5–7]. In biosensor applications, conducting polymers have been one of the attractive materials as they are utilized for the immobilization of biomolecules and improve the electron transfer rate [8]. The combination of conducting polymers and nanomaterials, *e.g.*, carbon materials, metal nanoparticles, has been focused on developing a new generation of electrochemical biosensors [9–12]. The advantages of the combination, especially with carbon nanotubes (CNTs), including the achievement of large electroactive surface area, increasing electron transfer performance, electrical conductivity, and mechanical properties had been reported [13, 14]. Carbon materials, especially CNTs and graphenes, have been studied for utilization of the direct electron transfer to enzyme active site, which could act as molecular wires capable of tunneling electrons from the enzyme active site to the electrode [15–17]. CNTs have been intensively and extensively studied in many applications, including sensors [15, 18, 19], environmental treatment [20, 21], antibacterial applications [22], and supercapacitors [5] due to their high surface area, high thermal capacity,

*Corresponding author, e-mail: saengrawee.s@cmu.ac.th

mechanical stability, great electrochemical property [23, 24]. In addition, CNTs exhibited a unique structure which led to certain electrical and electrochromic properties for suitable use as transducers to generate the signal upon detection of the target molecules [25–27]. They also could serve as support materials for the non-covalent absorption of biomolecules in biosensor applications [28, 29]. The limitation of using CNTs in polymer composites was the dispersion and compatibility of CNTs with the polymer matrices [30]. The decreasing of graphene layers in CNTs leads to increasing of aggregation. The order of aggregation increment is multi-walled, double-walled, and single-walled CNTs, respectively [31]. Moreover, to overcome this limitation, the functionalization of CNTs by covalent or non-covalent surface modification and filling of CNTs had been an attractive method to facilitate in various studies [25, 32–34]. We, therefore, employed carboxylic acid-functionalized multi-walled CNTs in this study. Furthermore, the toxicological effects of CNTs, including cytotoxicity, oxidative stress, or genotoxicity, could be considered as one of the limitations for CNTs usage. The metal contaminants of CNTs, *e.g.*, nickel or iron which used in CNTs synthesis, could cause cytotoxicity and oxidative stress of studied cells. Typically, the commercial CNTs have been synthesized by chemical vapor deposition (CVD) as the metals have not been used in the synthesis [35, 36]. We, therefore, employed the commercially available CNTs synthesized by CVD.

The development of electrochemical biosensors for the detection of various biomolecules such as DNA [37, 38], glucose [39, 40], biomarkers [41, 42] had been reported. Especially, enzyme-based electrochemical biosensors or bioelectrodes have been extensively studied. The enzyme could act as a biocatalyst that transfers electrons to the electrode. In addition, the redox mediators such as conducting polymers and composites could utilize electron transfer to the electrode. The common electrodes, including glassy carbon [43, 44], gold [28], indium tin oxide [23, 45], fluorine-doped indium tin oxide [46, 47] electrodes, have been normally used to fabricate the electrochemical biosensor electrodes. In addition, a screen-printed electrode (SPE) had become an attractive electrode due to its suitability for microvolume usage, the ability for chemical modification, disposability, ease of production, and opportunity for incorporation with nanomaterials [17, 48, 49]. We, therefore, selected the SPE for the fabrication of the electrochemical glucose biosensor in this study. The performance of the electrodes or biosensors had been affected by their morphologies at nanoscale. Therefore, the surface morphology of electrodes or biosensors could be adjusted by the film fabrication process. The electrospinning method has been a promising method for producing polymeric nanofibers in various applications, including sensors [46, 50, 51], antibacterial surfaces [52], drug delivery, or pharmaceutical applications [53, 54], lithium-ion battery [55]. In biosensor application, the electrospun nanofibers with high porosity and high surface area to volume ratio on the electrodes can utilize as the matrices for immobilization of biomolecules. Recently, the biosensors based on electrospun nanofibers showed higher sensitivity and selectivity than the flat film sensor [56, 57]. In this study, we fabricated the electrochemical glucose biosensor based on electrospun nanofibers of the conducting polymer composite.

Diabetes has become one of the major diseases with a high death rate worldwide. The development of glucose biosensors with inexpensive, easy-to-use, high sensitivity and selectivity is nowadays, therefore important for monitoring glucose [46]. This study aims to develop the electrochemical glucose biosensor based on conducting polymer, *i.e.*, poly(3-aminobenzylamine) (PABA)/functionalized multi-walled carbon nanotubes (f-CNTs) composite. To the best of our knowledge, the composite of this polyaniline derivative (PABA) with f-CNTs for electrochemical glucose biosensors has never been reported. The electrospun fiber film of PABA/f-CNTs composite was fabricated on SPE, which was then immobilized with glucose oxidase (GOD) for use as an electrochemical glucose biosensor. The electrospun fiber film was characterized by attenuated total reflectance-Fourier transform infrared spectroscopy (ATR-FTIR), X-ray diffraction (XRD), and X-ray photoelectron spectroscopy (XPS), and field emission–scanning electron microscopy (FE-SEM). The electrochemical properties of the obtained glucose biosensor were investigated using cyclic voltammetry (CV), amperometry, and electrochemical impedance spectroscopy (EIS). Figure 1 represents the schematic diagram of the electrochemical glucose biosensor based on the electrospun fiber of PABA/f-CNTs. The presence of f-CNTs in the composite could improve the performance of the developed glucose biosensor in terms of sensitivity, selectivity and stability.

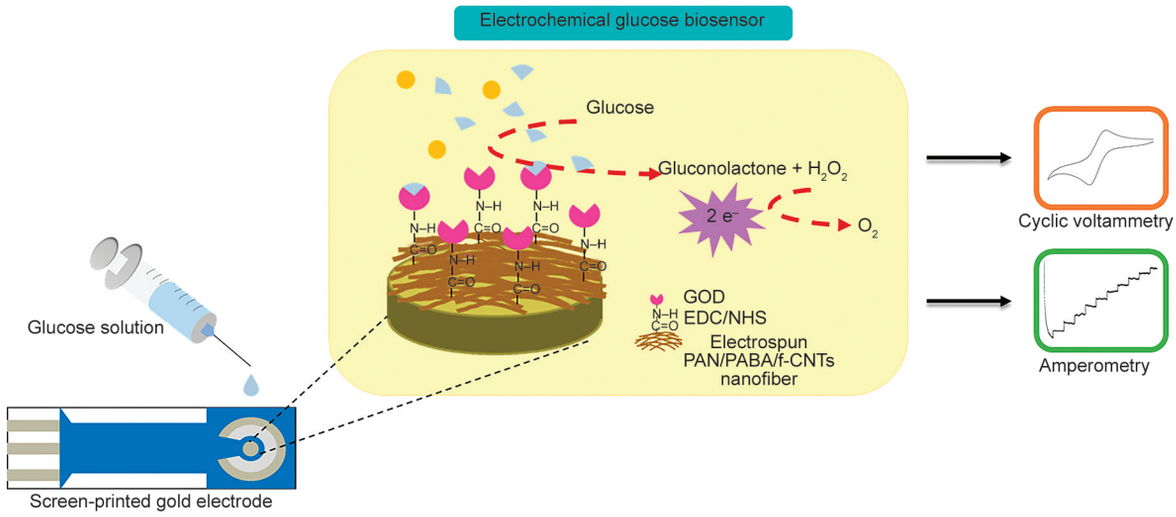

Figure 1. Schematic diagram represents the fabrication of the electrochemical glucose biosensor based on electrospun PABA/f-CNTs.

2. Experimental

2.1. Materials

D-glucose, 3-aminobenzyl amine (ABA), 4-(2-hydroxyethyl) piperazine-1-ethanesulfonic acid (HEPES), polyacrylonitrile (PAN), 1-ethyl-3-(3-dimethylaminopropyl) carbodiimide (EDC), *N*-hydroxyl succinimide (NHS), dimethylformamide (DMF), and dopamine (DA) were purchased from Sigma-Aldrich (Darmstadt, Germany). Ascorbic acid (AA) was purchased from Poch (Gliwice, Poland). Glucose oxidase (GOD) and uric acid (UA) were purchased from Bio Basic (Ontario, Canada). Potassium hexacyanoferrate ($K_3Fe(CN)_6$) was purchased from Scharlau (Barcelona, Spain). All chemicals were used as received without further purification. All aqueous solutions were prepared with DI water. Screen-printed electrode (BVT-AC1) with silver/silver chloride (Ag/AgCl) as reference electrode, gold (Au) as working, and counter electrodes were purchased from PalmSens BV (Houten, Netherlands) and cleaned prior to use. The PABA was synthesized according to our previous study [47], and the f-CNTs were prepared according to a previous study [34].

2.2. Fabrication of electrospun PABA/f-CNTs composite fiber film

The electrospun PABA/f-CNTs composite fiber film was prepared on SPE with the following procedure. The PABA/f-CNTs solution was firstly prepared by dissolving PABA (3% w/v), f-CNTs (0.05% w/v), and PAN (5% w/v) in DMF. The solution was sonicated for 30 min and centrifuged at 4000 rpm for 30 min. The obtained solution was then freshly stirred for 1 h before use for fabrication of electrospun PABA/f-CNTs composite fiber film. The optimized electrospinning condition was the voltage of 15 kV, feeding rate of 1.0 ml/h, the distance between the syringe and the collector (*i.e.*, SPE) of 15 cm, and period time of 10 min. The obtained PABA/f-CNTs composite fiber film was immobilized with GOD by immersing in 0.1 M EDC/0.4 M NHS aqueous solution for 10 minutes to activate the PABA/f-CNTs surface [58] and subsequently immersing in GOD (1 mg/ml in HEPES buffer) for 10 minutes to obtain PABA/f-CNTs/GOD film on SPE [59]. The PABA/f-CNTs/GOD was further employed for electrochemical detection of glucose.

2.3. Characterization of PABA/f-CNTs composite

The obtained PABA/f-CNTs composite was characterized with various techniques prior to employing for electrochemical detection of glucose. The chemical constituents were investigated using ATR-FTIR (Bruker Tensor 27, Billerica, MA, USA), XRD (Rigaku Smartlab, Akishima, Japan), and XPS (AXIS ultra DLD spectrometer, Manchester, UK). The surface morphology was characterized using FE–SEM (JEOL JSM-6335F, Tokyo, Japan).

2.4. Electrochemical detection of glucose

All electrochemical experiments, including CV, amperometry, and EIS, were performed using a ready-to-go potentiostat Sensit Smart (PalmSens BV, Houten, Netherlands) with the three-electrode system on SPE (Ag/AgCl as reference electrode, Au as

working and counter electrodes). The electrochemical properties of the electrospun fibers were investigated using CV at various scan rates (20–400 mV/s) with a potential range of –0.2 to 0.7 V in 10 mM HEPES buffer (pH 7.0) containing 5 mM $K_3Fe(CN)_6$ and 0.1 M KCl. The surface resistance of the obtained electrospun fiber films was studied using EIS measurement in the buffer at an applied voltage of 0.1 V and frequency range of 0.1 to 100 kHz. The sensitivity of the obtained glucose biosensor based on electrospun PABA/f-CNTs/GOD was obtained by performing the amperometric experiment with successive adding of various concentrations of glucose (0.56–2.8 mM) into the buffer at a constant applied potential of 0.7 V. In addition, the amperometric responses upon adding of the common interferences (*i.e.*, dopamine, ascorbic acid, uric acid) at a constant applied potential of 0.7 V were obtained for selectivity experiment. The stability of the glucose sensors was also investigated using amperometry at constant applied potential of 0.7 V for 14 days.

3. Results and discussion

3.1. Characterization of PABA/f-CNTs composite

The electrospun fiber films of PABA and PABA/f-CNTs composite were fabricated with the optimized electrospinning condition, which was the voltage of 15 kV, feeding rate of 1.0 ml/h, period time of 10 min, and distance between the syringe and the collector of 15 cm. The prepared electrospun fiber films were characterized with various techniques including, ATR-FTIR spectroscopy, XPS, XRD, and FE-SEM. The functional groups and chemical constituents were studied by ATR–FTIR spectroscopy. The ATR-FTIR spectra of PABA, f-CNTs, and PABA/f-CNTs composite films are shown in Figure 2. The broad band at around 3400 cm^{-1} and peak at 1645 cm^{-1} of f-CNTs spectrum indicated the O–H and C–O stretching vibrations of COOH groups on the surface of f-CNTs [34]. The PABA and PABA/f-CNTs composite films showed identical spectra. The peak at 2930 cm^{-1} was assigned to the C–H stretching of the aromatic ring on the PABA chain. The C=C of the aromatic ring and C–N stretching of PABA presented the peaks at 1450 and 1350 cm^{-1}, respectively [47]. The presence of f-CNTs in the PABA/f-CNTs composite film was not clearly observed using FT-IR spectroscopy. However, other characterization techniques, *i.e.*, XPS and XRD,

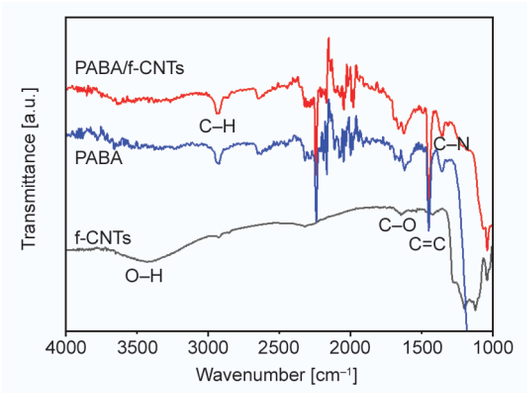

Figure 2. ATR-FTIR spectra of PABA, f-CNTs, and PABA/f-CNTs composite films.

were then employed to confirm the presence of f-CNTs in the PABA/f-CNTs composite film.

XPS measurement was performed to further analyze the chemical constituents of the electrospun films. Figure 3 represents the XPS spectra of f-CNTs, PABA, and PABA/f-CNTs films. The survey spectra in Figure 3a showed the C1s, N1s, and O1s at about 285, 400, and 532 eV, respectively, for f-CNTs, PABA, and PABA/f-CNTs films. The presence of oxygen in PABA film was probably from the contamination during the preparation process which was caused by the environmental contact and water adsorption upon storage [10]. The high-resolution C1s spectrum of f-CNTs (Figure 3b) represented the C–C(sp^2) of hexagon wall of CNTs, C–C(sp^3) of the defect in the aromatic structure of CNTs, C–O, C=O, O–C=O at a binding energy of 284.2, 285.0, 285.8, 287.0 and 287.6 eV, respectively [20]. Figure 3c shows the high-resolution spectra of PABA film. The C1s peaks appeared at 283.3, 285.0, 286.1, and 287.6 eV corresponding to C=C, C–N/C=N, C–$N^{\bullet+}$/C=$N^{\bullet+}$, and C=N of benzenoid and quinoid structures in the PABA chain. In addition, the N1s spectrum presented 2 peaks at 399.0 and 400.6 eV, which contributed to –N=, –NH/–NH_2, and –$N^{\bullet+}$– species in PABA structure [60]. The high-resolution C1s and N1s spectra of PABA/f-CNTs film are presented in Figure 3d. The contributions of C1s and N1s peaks are identical to PABA film. However, the proportion of –$N^{\bullet+}$– was observed to be higher than PABA, which could be proof for interaction between PABA and f-CNTs in the composite film [61]. This interaction led to the enhancement of electrochemical characteristics of the PABA/f-CNTs composite, which will be investigated in the next title.

XRD patterns of f-CNTs, PABA, and PABA/f-CNTs films are shown in Figure 4. The f-CNTs presented

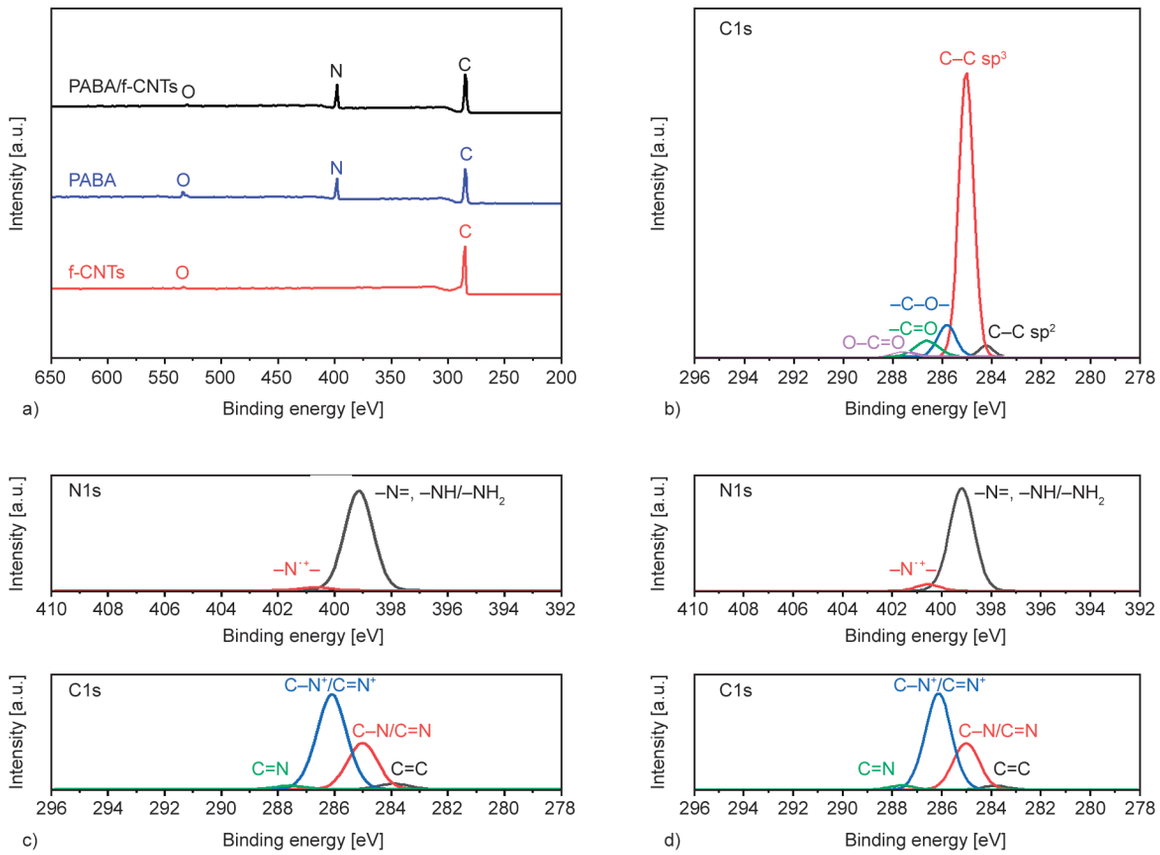

Figure 3. XPS a) survey spectra and high-resolution spectra of b) f-CNTs, c) PABA, and d) PABA/f-CNTs films.

a broad peak of the (002) plane at an angle of 2θ = 25.7° which indicated the graphitic carbon in f-CNTs structure [62, 63]. The broad peak of PABA was observed at an angle of 2θ = 22.6° which attributed to amorphous structures of benzenoid and quinoid rings of the PABA chain [64, 65]. This broad peak of the PABA in PABA/f-CNTs films was slightly shifted to a higher angle of 2θ = 23.6° which could be implied that the f-CNTs in the composite could decrease the interlayer spacing due to the interaction of PABA and CNTs. This result could confirm the presence of f-CNTs in the composite. The peak at an angle of 2θ = 17.0° was from the (100) plane of PAN [66] which was employed for electrospun film formation. In the case of conducting polymers, especially polyaniline and its derivatives, the production of the electrospun fiber was difficult because of the rigid backbone and lack of elastic properties [10]. The addition of non-conductive polymers such as PAN or polyacrylic acid (PAA) could therefore improve the formation of the electrospun conducting polymer fiber.

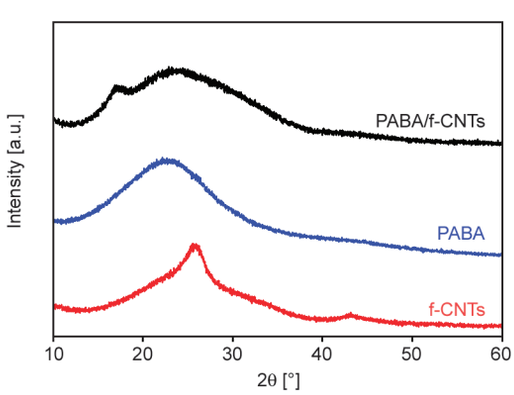

Figure 4. XRD patterns of f-CNTs, PABA and PABA/f-CNTs films.

To investigate the morphology of the prepared electrospun films, the cross-section view of the films was performed using FE-SEM. Figure 5 presents the FE-SEM images of PABA (Figure 5a) and PABA/f-CNTs (Figure 5b) films. It can be observed that the surfaces of the PABA and PABA/f-CNTs fibers were smooth, uniform, and bead-free, with the average diameters of the fibers were 106±20 and 150±24 nm, respectively. The incorporation of f-CNTs in the composite can cause the increase of PABA/f-CNTs fiber size [10]. The addition of f-CNTs could influence the volatility and viscosity of the composite solution employed in the electrospinning process, which results in an increase in the fiber diameter.

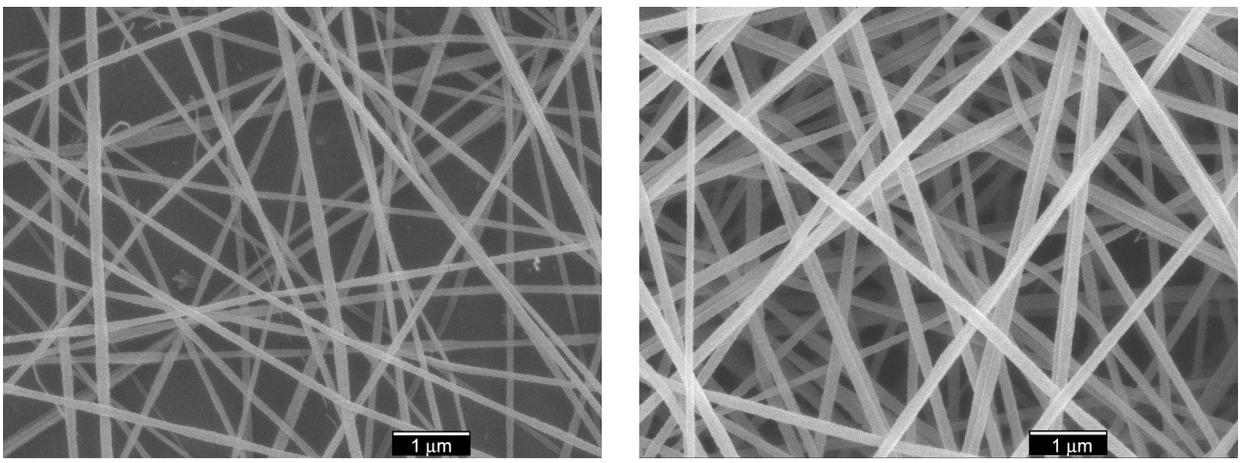

Figure 5. FE-SEM images of a) PABA and b) PABA/f-CNTs films.

3.2. Electrochemical characteristics of the electrospun films

The electrochemical characteristics of the electrospun PABA and PABA/f-CNTs films on SPE were investigated using CV and EIS. The CV measurement was performed in the potential range of –0.2 to 0.7 V at various scan rates (20–400 mV/s) prior to use as an electrochemical glucose biosensor. The $K_3Fe(CN)_6$ (5 mM) containing KCl (0.1 M) in HEPES buffer solution (pH 7) was employed as a redox mediator in this experiment. The CV responses of PABA and PABA/f-CNTs films are presented in Figure 6a and Figure 6b, respectively. The PABA and PABA/f-CNTs films presented the identical CV responses with the average difference of anodic and cathodic peak potentials (ΔE_p) of 0.25 V. Figure 6c

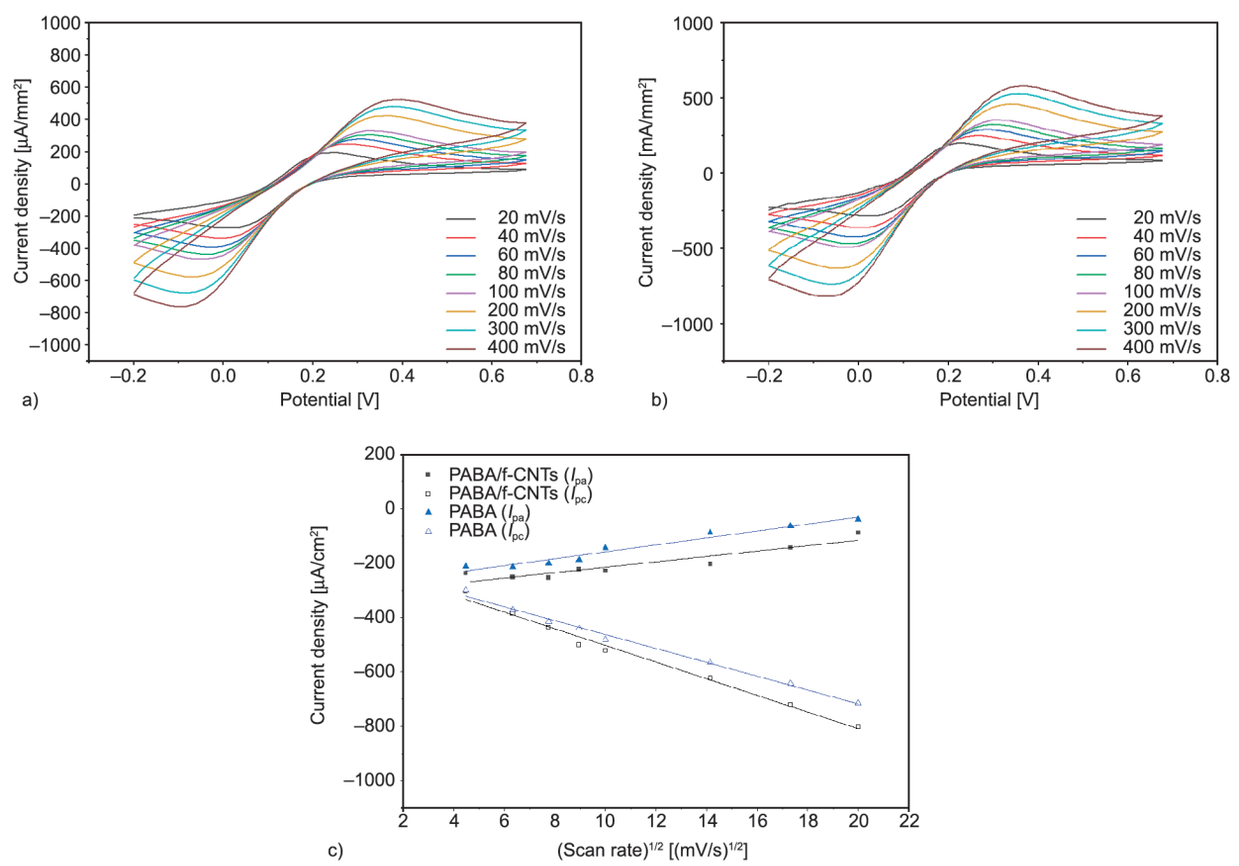

Figure 6. Cyclic voltammograms of a) PABA, b) PABA/f-CNTs films performed in HEPES buffer solution (pH 7) containing $K_3Fe(CN)_6$ (5 mM) and KCl (0.1 M) at various scan rates and c) linear relationship expression of peak current (I_p) *versus* square root of the scan rate ($v^{1/2}$).

showed the linear relationship expressions of anodic current peak height (I_{pa}) and cathodic current peak height (I_{pc}) versus square root of the scan rate ($v^{1/2}$). The linear expressions indicated the diffusion control at the electrode surface [10, 47].

To further study the electrochemical property of the fabricated electrospun films, EIS measurement was employed to investigate the impedance of the different electrodes, *i.e.*, PABA and PABA/f-CNTs composite films [67]. The obtained Nyquist plots with the Randles equivalent circuit model of PABA and PABA/f-CNTs electrodes in HEPES buffer at an applied voltage of 0.1 V and frequency range of 0.1 to 100 kHz are shown in Figure 7. The charge or electron transfer resistance (R_{ct}) of the electrodes was calculated from the semicircle of the obtained spectra. The larger semicircle of PABA exhibited the R_{ct} of 4,810 Ω, whereas the PABA/f-CNTs electrode showed the R_{ct} of 3,100 Ω. The surface resistivity of the PABA/f-CNTs composite was decreased due to the presence of the f-CNTs could increase the direct electron transition and influence the electroactivity of the electrode [46]. The CV and EIS results can therefore confirm the presence of f-CNTs in the electrospun PABA/f-CNTs composite fiber electrode.

3.3. Amperometric detection of glucose

For electrochemical detection of glucose, the fabricated electrospun PABA and PABA/f-CNTs films on SPE were immobilized with GOD for selective detection of glucose. In electrochemical enzyme-based glucose biosensor, the GOD was chosen as a model enzyme because of its stability, inexpensive and practical usage [68]. The oxidized GOD was also utilized as the catalyst for glucose oxidation to gluconolactone and hydrogen peroxide at an anodic potential higher than 0.6 V *vs*. Ag/AgCl electrode. We, therefore, used the potential of 0.7 V in the amperometric experiment to ensure the electrochemical oxidation of glucose. The reduction of hydrogen peroxide was then occurred, which resulted in the current flow [9, 69]. The amperometric responses for detection of glucose (0.56–2.8 mM) in HEPES buffer at a constant applied potential of 0.7 V are shown in Figure 8. The current responses of PABA and PABA/f-CNTs electrodes were increased upon successive addition of glucose into the buffer solution, whereas the current responses of the bare SPE, PABA, and PABA/f-CNTs without immobilized GOD were observed to be constant. The results could demonstrate and confirm the role of GOD for the selective detection of glucose. The current response of the PABA/f-CNTs electrode was obviously greater than that of PABA, which demonstrated that the presence of f-CNTs could enhance the electroactivity of PABA for the detection of glucose. The carboxylic group of f-CNTs could create the reactive sites at the sidewall and end of f-CNTs which utilize the interaction with the target molecule. The sensitivities of the electrodes were calculated to be 0.21 and 0.40 $\mu A \cdot mm^{-2} \cdot mM^{-1}$ with a limit of detection (LOD) of 0.083 and 0.067 mM in the linear range of 0.56–2.8 mM (R^2 = 0.95) for PABA and PABA/ f-CNTs, respectively. These results emphasized that the presence of f-CNTs could improve the sensitivity and LOD of the PABA/f-CNTs electrode. Table 1 presents the

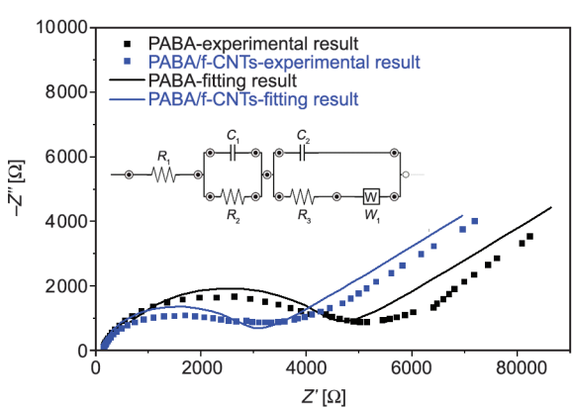

Figure 7. Nyquist plots with the equivalent circuit model of PABA and PABA/f-CNTs electrodes in HEPES buffer at an applied voltage of 0.1 V and frequency range of 0.1 to 100 kHz.

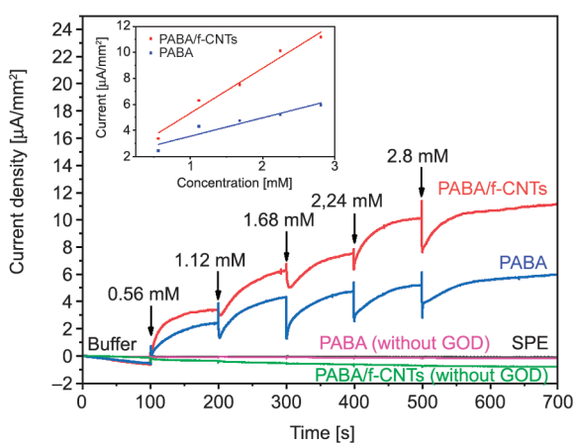

Figure 8. Amperometric responses of PABA and PABA/f-CNTs electrodes upon successive addition of glucose (0.56–2.8 mM) in HEPES buffer at a constant applied potential of 0.7 V. Inset is the corresponding calibration curves.

Table 1. Comparison of electrochemical glucose biosensors based on conducting polymers/CNTs.

Electrode	Sensitivity [$\mu A \cdot mm^{-2} \cdot mM^{-1}$]	LOD [mM]	Linear range [mM]	References
CH-GOD/PPy-Nf-f-CNTs/GCE	28.60	0.005	0.01–4.70	[9]
SWNT-PPy-GOD/Pt	7.06	–	1–50	[12]
Nf-silica-CNT-PANI/GOD/ITO	5.01	–	1–10	[70]
GOD/PANI/CH-CNTs/Au	0.21	0.100	1–20	[71]
GOD/n-TiO_2/PANI-active carbon/GCE	0.063	0.018	0.02–6.00	[72]
PABA/f-CNTs/Au	0.40	0.067	0.56–2.80	This work

Abbreviation: glassy carbon electrode (GCE), Nafion (Nf), Chitosan (CH), single-walled carbon nanotube (SWNT), polypyrrole (PPy), polyaniline (PANI), indium tin oxide (ITO).

comparison of the PABA/f-CNTs electrode in this study with the previously reported studies.

3.4. Interference, stability and reproducibility tests

The common interferences, *i.e.*, ascorbic acid (AA), uric acid (UA), and dopamine (DA), could affect the electrochemical detection of glucose because they could produce undesirable electrochemical signal [68]. The selectivity experiment under the normal level of these interferences was performed using amperometry. The amperometric response of PABA/f-CNTs electrode for detection of glucose (5.6 mM), AA (50 µM), UA (0.4 µM), and DA (1 µM) in HEPES buffer at a constant applied potential of 0.7 V is shown in Figure 9. It could be obviously observed that glucose exhibited a higher response than the interferences due to the immobilization of GOD catalyst onto the PABA/f-CNTs electrode utilized the selective detection of glucose in the common interferences.

To evaluate the stability of the fabricated electrodes, the fabricated electrodes were stored at room temperature without humidity for up to 14 days. The amperometric responses of the electrodes upon detection of glucose were measured every two-day interval for 1 week. The current response of the PABA/f-CNTs electrode retained about 80% after 1 week, whereas the current response of the PABA electrode retained only about 22% after 3 days (Figure 10). However, the current responses of both electrodes were dropped to almost zero after 2 weeks, *i.e.*, zero for PABA and about 10% for PABA/f-CNTs. These results indicated that the presence of f-CNTs in the PABA/f-CNTs could improve the stability of the electrode. In addition, the reproducibility of the PABA/f-CNTs biosensor electrode was examined by measuring the amperometric current responses of five similar independently fabricated electrodes in 1.0 mM glucose. A low relative standard deviation (RSD) of 2.4% was obtained, which indicated great reproducibility of the PABA/f-CNTs electrode.

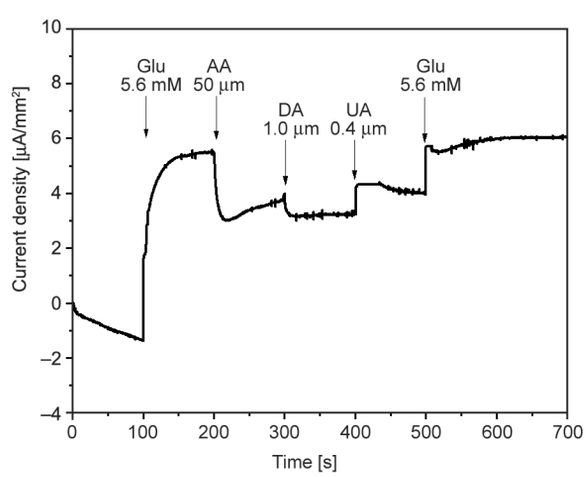

Figure 9. Amperometric response of PABA/f-CNTs electrode upon successive addition of glucose and interferences (UA, AA, DA) in HEPES buffer at a constant potential of 0.7 V.

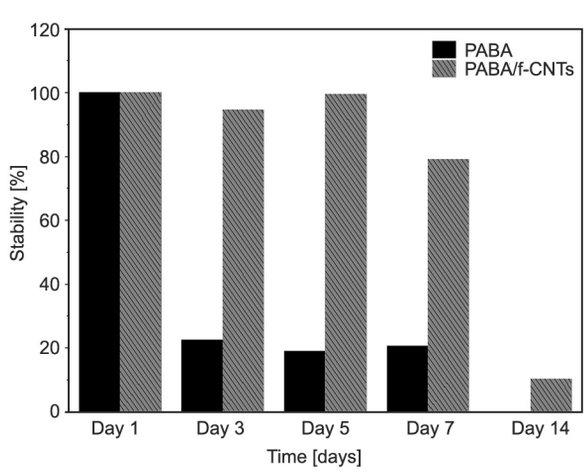

Figure 10. Stability histograms of PABA and PABA/f-CNTs electrodes upon electrochemical detection of glucose.

4. Conclusions

The electrospun fiber film of conducting polymer/carbon nanotubes (PABA/f-CNTs) composite was successfully fabricated on SPE for use as an electrochemical glucose biosensor. The electrochemical characteristics of the PABA/f-CNTs confirmed that the presence of f-CNTs in the composite utilized the enhancement of electrochemical properties of PABA upon detection of glucose at various concentrations (0.56–2.8 mM) and under common interferences. The amperometry was employed to investigate the sensitivity, selectivity, and stability of the prepared electrospun PABA/f-CNTs electrode. It can be concluded that the PABA/f-CNTs electrode represented high selectivity, the sensitivity of 0.40 $\mu A \cdot mm^{-2} \cdot mM^{-1}$ with LOD of 0.067 mM in the linear range of 0.56–2.8 mM and good stability up to 1 week with the current response retained about 80%. This obtained electrode could be developed as a sensing platform for future use in real sample analysis.

Acknowledgements

The work was supported by the Center of Excellence in Materials Science and Technology, Chiang Mai University.

References

[1] Salam F., Tothill I. E.: Detection of Salmonella typhimurium using an electrochemical immunosensor. Biosensors and Bioelectronics, **24**, 2630–2636 (2009). https://doi.org/10.1016/j.bios.2009.01.025

[2] Lange U., Roznyatovskaya N. V., Mirsky V. M.: Conducting polymers in chemical sensors and arrays. Analytica Chimica Acta, **614**, 1–26 (2008). https://doi.org/10.1016/j.aca.2008.02.068

[3] Cui M., Song Z., Wu Y., Guo B., Fan X., Luo X.: A highly sensitive biosensor for tumor maker alpha fetoprotein based on poly(ethylene glycol) doped conducting polymer PEDOT. Biosensors and Bioelectronics, **79**, 736–741 (2016). https://doi.org/10.1016/j.bios.2016.01.012

[4] Abdulla S., Mathew T. L., Pullithadathil B.: Highly sensitive, room temperature gas sensor based on polyaniline-multiwalled carbon nanotubes (PANI/MWCNTs) nanocomposite for trace-level ammonia detection. Sensors and Actuators B, **221**, 1523–1534 (2015). https://doi.org/10.1016/j.snb.2015.08.002

[5] Kim J-G., Lee D-M., Jung J. Y., Kim M. J., Khil M-S., Jeong H. S., Kim N. D.: Hybrid polyaniline/liquid crystalline CNT fiber composite for ultimate flexible supercapacitors. ACS Applied Energy Materials, **4**, 1130–1142 (2021). https://doi.org/10.1021/acsaem.0c02217

[6] Porcarelli L., Shaplov A. S., Bella F., Nair J. R., Mecerreyes D., Gerbaldi C.: Single-ion conducting polymer electrolytes for lithium metal polymer batteries that operate at ambient temperature. ACS Energy Letters, **1**, 678–682 (2016). https://doi.org/10.1021/acsenergylett.6b00216

[7] Liu T., Finn L., Yu M., Wang H., Zhai T., Lu X., Tong Y., Li Y.: Polyaniline and polypyrrole pseudocapacitor electrodes with excellent cycling stability. Nano Letter, **14**, 2522–2527 (2014). https://doi.org/10.1021/nl500255v

[8] Azimi S., Farahani A., Sereshti H.: Plasma-functionalized highly aligned CNT-based biosensor for point of care determination of glucose in human blood plasma. Electroanalysis, **32**, 394–403 (2020). https://doi.org/10.1002/elan.201800895

[9] Shrestha B. K., Ahmad R., Mousa H. M., Kim I-G., Kim J. I., Neupane M. P., Park C. H., Kim C. S.: High-performance glucose biosensor based on chitosan-glucose oxidase immobilized polypyrrole/Nafion/functionalized multi–walled carbon nanotubes bio-nanohybrid film. Journal of Colloid and Interface Science, **482**, 39–47 (2016). https://doi.org/10.1016/j.jcis.2016.07.067

[10] Ratlam C., Phanichphant S., Sriwichai S.: Development of dopamine biosensor based on polyaniline/carbon quantum dots composite. Journal of Polymer Research, **27**, 183 (2020). https://doi.org/10.1007/s10965-020-02158-6

[11] Cui X., Li C. M., Zang J., Zhou Q., Gan Y., Bao H., Guo J., Lee V. S., Moochhala S. M.: Biocatalytic generation of Ppy-enzyme-CNT nanocomposite: From network assembly to film growth. The Journal of Physical Chemistry C, **111**, 2025–2031 (2007). https://doi.org/10.1021/jp0671594

[12] Shirsat M. D., Too C. O., Wallace G. G.: Amperometric glucose biosensor on layer by layer assembled carbon nanotube and polypyrrole multilayer film. Electroanalysis, **20**, 150–156 (2008). https://doi.org/10.1002/elan.200704028

[13] le Goff A., Holzinger M., Cosnier S.: Enzymatic biosensors based on SWCNT-conducting polymer electrodes. Analyst, **136**, 1279–1287 (2011). https://doi.org/10.1039/c0an00904k

[14] Alba N., Du Z., Catt K., Kozai T., Cui X.: *In vivo* electrochemical analysis of a PEDOT/MWCNT neural electrode coating. Biosensors, **5**, 618–646 (2015). https://doi.org/10.3390/bios5040618

[15] Liu J., Chou A., Rahmat W., Paddon-Row M. N., Gooding J. J.: Achieving direct electrical connection to glucose oxidase using aligned single walled carbon nanotube arrays. Electroanalysis, **17**, 38–46 (2005). https://doi.org/10.1002/elan.200403116

[16] Kang X., Wang J., Wu H., Aksay I. A., Liu J., Lin Y.: Glucose oxidase-graphene-chitosan modified electrode for direct electrochemistry and glucose sensing. Biosensors and Bioelectronics, **25**, 901–905 (2009). https://doi.org/10.1016/j.bios.2009.09.004

[17] Kong F-Y., Gu S-X., Li W-W., Chen T-T., Xu Q., Wang W.: A paper disk equipped with graphene/polyaniline/Au nanoparticles/glucose oxidase biocomposite modified screen-printed electrode: Toward whole blood glucose determination. Biosensors and Bioelectronics, **56**, 77–82 (2014). https://doi.org/10.1016/j.bios.2013.12.067

[18] Kress G. J., Shu H-J., Yu A., Taylor A., Benz A., Harmon S., Mennerick S.: Fast phasic release properties of dopamine studied with a channel biosensor. Journal of Neuroscience, **34**, 11792–11802 (2014). https://doi.org/10.1523/jneurosci.2355-14.2014

[19] Buber E., Kesik M., Soylemez S., Toppare L.: A biosensing platform utilizing a conjugated polymer, carbon nanotubes and PAMAM combination. Journal of Electroanalytical Chemistry, **799**, 370–376 (2017). https://doi.org/10.1016/j.jelechem.2017.06.043

[20] Wang H., Zhou A., Peng F., Yu H., Yang J.: Mechanism study on adsorption of acidified multiwalled carbon nanotubes to Pb(II). Journal of Colloid and Interface Science, **316**, 277–283 (2007). https://doi.org/10.1016/j.jcis.2007.07.075

[21] Li Y-H., Wang S., Luan Z., Ding J., Xu C., Wu D.: Adsorption of cadmium(II) from aqueous solution by surface oxidized carbon nanotubes. Carbon, **41**, 1057–1062 (2003). https://doi.org/10.1016/S0008-6223(02)00440-2

[22] Thampi V. V. A., Thanka Rajan S., Anupriya K., Subramanian B.: Functionalization of fabrics with PANI/CuO nanoparticles by precipitation route for anti-bacterial applications. Journal of Nanoparticle Research, **17**, 57 (2015). https://doi.org/10.1007/s11051-014-2853-9

[23] Talib N. A. A., Salam F., Yusof N. A., Alang Ahmad S. A., Sulaiman Y.: Optimization of peak current of poly (3,4-ethylenedioxythiophene)/multi-walled carbon nanotube using response surface methodology/central composite design. RSC Advances, **7**, 11101–11110 (2017). https://doi.org/10.1039/c6ra26135c

[24] Tarley C. R. T., Santos V. S., Baêta B. E. L., Pereira A. C., Kubota L. T.: Simultaneous determination of zinc, cadmium and lead in environmental water samples by potentiometric stripping analysis (PSA) using multiwalled carbon nanotube electrode. Journal of Hazardous Materials, **169**, 256–262 (2009). https://doi.org/10.1016/j.jhazmat.2009.03.077

[25] Tilmaciu C. M., Morris M. C.: Carbon nanotube biosensors. Frontiers in Chemistry, **3**, 59 (2015). https://doi.org/10.3389/fchem.2015.00059

[26] Balasubramanian K., Burghard M.: Chemically functionalized carbon nanotubes. Small, **1**, 180–192 (2005). https://doi.org/10.1002/smll.200400118

[27] Zhao Q., Gan Z., Zhuang Q.: Electrochemical sensors based on carbon nanotubes. Electroanalysis, **14**, 1609–1613 (2002). https://doi.org/10.1002/elan.200290000

[28] Su L., Gao F., Mao L.: Electrochemical properties of carbon nanotube (CNT) film electrodes prepared by controllable adsorption of CNTs onto an alkanethiol monolayer self-assembled on gold electrodes. Analytical Chemistry, **78**, 2651–2657 (2006). https://doi.org/10.1021/ac051997x

[29] Barsan M. M., Carvalho R. C., Zhong Y., Sun X., Brett C. M. A.: Carbon nanotube modified carbon cloth electrodes: Characterisation and application as biosensors. Electrochimica Acta, **85**, 203–209 (2012). https://doi.org/10.1016/j.electacta.2012.08.048

[30] Sanip S. M., Ismail A. F., Goh P. S., Soga T., Tanemura M., Yasuhiko H.: Gas separation properties of functionalized carbon nanotubes mixed matrix membranes. Separation and Purification Technology, **78**, 208–213 (2011). https://doi.org/10.1016/j.seppur.2011.02.003

[31] Liu X., Wang M., Zhang S., Pan B.: Application potential of carbon nanotubes in water treatment: A review. Journal of Environmental Sciences, **25**, 1263–1280 (2013). https://doi.org/10.1016/S1001-0742(12)60161-2

[32] O'Connell M. J., Boul P., Ericson L. M., Huffman C., Wang Y., Haroz E., Kuper C., Tour J., Ausman K. D., Smalley R. E.: Reversible water-solubilization of single-walled carbon nanotubes by polymer wrapping. Chemical Physics Letters, **342**, 265–271 (2001). https://doi.org/10.1016/s0009-2614(01)00490-0

[33] Tasis D., Tagmatarchis N., Georgakilas V., Prato M.: Soluble carbon nanotubes. Chemistry–A European Journal, **9**, 4000–4008 (2003). https://doi.org/10.1002/chem.200304800

[34] Wong K. C., Goh P. S., Ng B. C., Ismail A. F.: Thin film nanocomposite embedded with polymethyl methacrylate modified multi-walled carbon nanotubes for CO_2 removal. RSC Advances, **5**, 31683–31690 (2015). https://doi.org/10.1039/c5ra00039d

[35] Donaldson K., Aitken R., Tran L., Stone V., Duffin R., Forrest G., Alexander A.: Carbon nanotubes: A review of their properties in relation to pulmonary toxicology and workplace safety. Toxicological Sciences, **92**, 5–22 (2006). https://doi.org/10.1093/toxsci/kfj130

[36] Yang H., Liu C., Yang D., Zhang H., Xi Z.: Comparative study of cytotoxicity, oxidative stress and genotoxicity induced by four typical nanomaterials: The role of particle size, shape and composition. Journal of Applied Toxicology, **29**, 69–78 (2009). https://doi.org/10.1002/jat.1385

[37] Akhavan O., Ghaderi E., Rahighi R.: Toward single-DNA electrochemical biosensing by graphene nanowalls. ACS Nano, **6**, 2904–2916 (2012). https://doi.org/10.1021/nn300261t

[38] Ambrosi A., Pumera M.: Stacked graphene nanofibers for electrochemical oxidation of DNA bases. Physical Chemistry Chemical Physics, **12**, 8943–8947 (2010). https://doi.org/10.1039/C0CP00213E

[39] Shan D., Zhang J., Xue H-G., Ding S-N., Cosnier S.: Colloidal laponite nanoparticles: Extended application in direct electrochemistry of glucose oxidase and reagentless glucose biosensing. Biosensors and Bioelectronics, **25**, 1427–1433 (2010). https://doi.org/10.1016/j.bios.2009.10.046

[40] Gao H., Xiao F., Ching C. B., Duan H.: One-step electrochemical synthesis of PtNi nanoparticle-graphene nanocomposites for nonenzymatic amperometric glucose detection. ACS Applied Materials and Interfaces, **3**, 3049–3057 (2011). https://doi.org/10.1021/am200563f

[41] Haque A. M. J., Park H., Sung D., Jon S., Choi S-Y., Kim K.: An electrochemically reduced graphene oxide-based electrochemical immunosensing platform for ultrasensitive antigen detection. Analytical Chemistry, **84**, 1871–1878 (2012). https://doi.org/10.1021/ac202562v

[42] Wang X., Wang C., Qu K., Song Y., Ren J., Miyoshi D., Sugimoto N., Qu X.: Ultrasensitive and selective detection of a prognostic indicator in early-stage cancer using graphene oxide and carbon nanotubes. Advanced Functional Materials, **20**, 3967–3971 (2010). https://doi.org/10.1002/adfm.201001118

[43] Cheng G., Zhao J., Tu Y., He P., Fang Y.: A sensitive DNA electrochemical biosensor based on magnetite with a glassy carbon electrode modified by muti-walled carbon nanotubes in polypyrrole. Analytica Chimica Acta, **533**, 11–16 (2005). https://doi.org/10.1016/j.aca.2004.10.044

[44] Chen S., Yang W., Chen X.: Highly sensitive and selective determination of dopamine based on graphite nanosheet-Nafion composite film modified electrode. Electroanalysis, **22**, 908–911 (2010). https://doi.org/10.1002/elan.200900511

[45] Manesh K. M., Santhosh P., Gopalan A., Lee K-P.: Electrospun poly(vinylidene fluoride)/poly(aminophenylboronic acid) composite nanofibrous membrane as a novel glucose sensor. Analytical Biochemistry, **360**, 189–195 (2007). https://doi.org/10.1016/j.ab.2006.09.021

[46] Utarat P., Phanichphant S., Sriwichai S.: Preparation of electrospun poly(acrylic acid)/multiwalled carbon nanotubes composite nanofiber for glucose detection. Molecular Crystals and Liquid Crystals, **688**, 114–121 (2019). https://doi.org/10.1080/15421406.2019.1648032

[47] Panapimonlawat T., Phanichphant S., Sriwichai S.: Electrochemical dopamine biosensor based on poly(3-aminobenzylamine) layer-by-layer self-assembled multilayer thin film. Polymers, **13**, 1488 (2021). https://doi.org/10.3390/polym13091488

[48] Ping J., Wu J., Wang Y., Ying Y.: Simultaneous determination of ascorbic acid, dopamine and uric acid using high-performance screen-printed graphene electrode. Biosensors and Bioelectronics, **34**, 70–76 (2012). https://doi.org/10.1016/j.bios.2012.01.016

[49] Bernalte E., Sánchez C. M., Gil E. P.: Determination of mercury in ambient water samples by anodic stripping voltammetry on screen-printed gold electrodes. Analytica Chimica Acta, **689**, 60–64 (2011). https://doi.org/10.1016/j.aca.2011.01.042

[50] Netsuwan P., Mimiya H., Baba A., Sriwichai S., Shinbo K., Kato K., Futao K., Phanichphant S.: Long-range surface plasmon resonance immunosensor based on water-stable electrospun poly(acrylic acid) fibers. Sensors and Actuators B: Chemical, **204**, 770–776 (2014). https://doi.org/10.1016/j.snb.2014.07.121

[51] Demirci Uzun S., Kayaci F., Uyar T., Timur S., Toppare L.: Bioactive surface design based on functional composite electrospun nanofibers for biomolecule immobilization and biosensor applications. ACS Applied Materials and Interfaces, **6**, 5235–5243 (2014). https://doi.org/10.1021/am5005927

[52] Kayaci F., Umu O. C. O., Tekinay T., Uyar T.: Antibacterial electrospun poly(lactic acid) (PLA) nanofibrous webs incorporating triclosan/cyclodextrin inclusion complexes. Journal of Agricultural and Food Chemistry, **61**, 3901–3908 (2013). https://doi.org/10.1021/jf400440b

[53] Canbolat M. F., Celebioglu A., Uyar T.: Drug delivery system based on cyclodextrin-naproxen inclusion complex incorporated in electrospun polycaprolactone nanofibers. Colloids and Surfaces B: Biointerfaces, **115**, 15–21 (2014). https://doi.org/10.1016/j.colsurfb.2013.11.021

[54] Szabó E., Démuth B., Nagy B., Molnár K., Farkas A., Szabó B., Balogh A., Hirsch E., Nagy B., Marosi Gy., Nagy Z. K.: Scaled-up preparation of drug-loaded electrospun polymer fibres and investigation of their continuous processing to tablet form. Express Polymer Letters, **12**, 436–451 (2018). https://doi.org/10.3144/expresspolymlett.2018.37

[55] Kim J. R., Choi S. W., Jo S. M., Lee W. S., Kim B. C.: Electrospun PVdF-based fibrous polymer electrolytes for lithium ion polymer batteries. Electrochimica Acta, **50**, 69–75 (2004). https://doi.org/10.1016/j.electacta.2004.07.014

[56] Wang X., Drew C., Lee S-H., Senecal K. J., Kumar J., Samuelson L. A.: Electrospun nanofibrous membranes for highly sensitive optical sensors. Nano Letters, **2**, 1273–1275 (2002). https://doi.org/10.1021/nl020216u

[57] Lee M., Kim T-I., Kim K-H., Kim J-H., Choi M-S., Choi H-J., Koh K.: Formation of a self-assembled phenylboronic acid monolayer and its application toward developing a surface plasmon resonance-based monosaccharide sensor. Analytical Biochemistry, **310**, 163–170 (2002). https://doi.org/10.1016/s0003-2697(02)00305-6

[58] Sriwichai S., Baba A., Phanichphant S., Shinbo K., Kato K., Kaneko F.: Electrochemically controlled surface plasmon resonance immunosensor for the detection of human immunoglobulin G on poly(3-aminobenzoic acid) ultrathin films. Sensors and Actuators B: Chemical, **147**, 322–329 (2010). https://doi.org/10.1016/j.snb.2010.03.031

[59] Sriwichai S., Janmanee R., Phanichphant S., Shinbo K., Kato K., Kaneko F., Yamamoto T., Baba A.: Development of an electrochemical-surface plasmon dual biosensor based on carboxylated conducting polymer thin films. Journal of Applied Polymer Science, **135**, 45641 (2017). https://doi.org/10.1002/app.45641

[60] Graf N., Yegen E., Gross T., Lippitz A., Weigel W., Krakert S., Terfort A., Unger W. E. S.: XPS and NEXAFS studies of aliphatic and aromatic amine species on functionalized surfaces. Surface Science, **603**, 2849–2860 (2009). https://doi.org/10.1016/j.susc.2009.07.029

[61] Marmisollé W. A., Maza E., Moya S., Azzaroni O.: Amine-appended polyaniline as a water dispersible electroactive polyelectrolyte and its integration into functional self-assembled multilayers. Electrochimica Acta, **210**, 435–444 (2016). https://doi.org/10.1016/j.electacta.2016.05.182

[62] Dhall S., Jaggi N., Nathawat R.: Functionalized multiwalled carbon nanotubes based hydrogen gas sensor. Sensors and Actuators A: Physical, **201**, 321–327 (2013). https://doi.org/10.1016/j.sna.2013.07.018

[63] Keerthi M., Boopathy G., Chen S-M., Chen T-W., Lou B-S.: A core-shell molybdenum nanoparticles entrapped f-MWCNTs hybrid nanostructured material based non-enzymatic biosensor for electrochemical detection of dopamine neurotransmitter in biological samples. Scientific Reports, **9**, 13075 (2019). https://doi.org/10.1038/s41598-019-48999-0

[64] Shi L., Wang X., Lu L., Yang X., Wu X.: Preparation of TiO_2/polyaniline nanocomposite from a lyotropic liquid crystalline solution. Synthetic Metals, **159**, 2525–2529 (2009). https://doi.org/10.1016/j.synthmet.2009.08.056

[65] Mostafaei A., Zolriasatein A.: Synthesis and characterization of conducting polyaniline nanocomposites containing ZnO nanorods. Progress in Natural Science: Materials International, **22**, 273–280 (2012). https://doi.org/10.1016/j.pnsc.2012.07.002

[66] Qiao M., Kong H., Ding X., Hu Z., Zhang L., Cao Y., Yu M.: Study on the changes of structures and properties of pan fibers during the cyclic reaction in supercritical carbon dioxide. Polymers, **11**, 402 (2019). https://doi.org/10.3390/polym11030402

[67] Kubendhiran S., Sakthinathan S., Chen S-M., Lee C. M., Lou B-S., Sireesha P., Su C.: Electrochemically activated screen printed carbon electrode decorated with nickel nano particles for the detection of glucose in human serum and human urine sample. International Journal of Electrochemical Science, **11**, 7934–7946 (2016). https://doi.org/10.20964/2016.09.11

[68] Biscay J., Rama E. C., García M. B. G., Carrazón J. M. P., García A. C.: Enzymatic sensor using mediator-screen-printed carbon electrodes. Electroanalysis, **23**, 209–214 (2010). https://doi.org/10.1002/elan.201000471

[69] Jose M. V., Marx S., Murata H., Koepsel R. R., Russell A. J.: Direct electron transfer in a mediator-free glucose oxidase-based carbon nanotube-coated biosensor. Carbon, **50**, 4010–4020 (2012). https://doi.org/10.1016/j.carbon.2012.04.044

[70] Gopalan A. I., Lee K. P., Ragupathy D., Lee S. H., Lee J. W.: An electrochemical glucose biosensor exploiting a polyaniline grafted multiwalled carbon nanotube/perfluorosulfonate ionomer–silica nanocomposite. Biometerials. **30**, 5999–6005 (2009). https://doi.org/10.1016/j.biomaterials.2009.07.047

[71] Wan D., Yuan S., Li G. L., Neoh K. G., Kang E. T.: Glucose biosensor from covalent immobilization of chitosan-coupled carbon nanotubes on polyaniline-modified gold electrode. ACS Applied Materials and Interfaces, **2**, 3083–3091 (2010). https://doi.org/10.1021/am100591t

[72] Tang W., Li L., Zeng X.: A glucose biosensor based on the synergistic action of nanometer-sized TiO_2 and polyaniline. Talanta, **131**, 417–423 (2015). https://doi.org/10.1016/j.talanta.2014.08.019